Received: 3 April 2024 | Accepted: 11 August 2024

DOI: 10.1111/bjh.19720

BJHaem
BRITISH JOURNAL OF HAEMATOLOGY

ORIGINAL PAPER

Haematological Malignancy – Biology

Modelling and drug targeting of a myeloid neoplasm with atypical 3q26/*MECOM* rearrangement using patient-specific iPSCs

Momoko Nakamura[1,2] | **Kazuhisa Chonabayashi**[1,2] | **Megumi Narita**[1] | **Yasuko Matsumura**[1] | **Misato Nishikawa**[1] | **Yotaro Ochi**[3] | **Yasuhito Nannya**[3,4] | **Masakatsu Hishizawa**[2,5] | **Daichi Inoue**[6] | **Ruud Delwel**[7,8] | **Seishi Ogawa**[3] | **Akifumi Takaori-Kondo**[2] | **Yoshinori Yoshida**[1]

[1]Department of Cell Growth and Differentiation, Center for iPS Cell Research and Application, Kyoto University, Kyoto, Japan

[2]Department of Hematology and Oncology, Graduate School of Medicine, Kyoto University, Kyoto, Japan

[3]Department of Pathology and Tumor Biology, Graduate School of Medicine, Kyoto University, Kyoto, Japan

[4]Division of Hematopoietic Disease Control, The Institute of Medical Science, The University of Tokyo, Tokyo, Japan

[5]Department of Hematology, Kyoto-Katsura Hospital, Kyoto, Japan

[6]Department of Hematology-Oncology, Institute of Biomedical Research and Innovation, Foundation for Biomedical Research and Innovation at Kobe, Kobe, Hyogo, Japan

[7]Department of Hematology, Erasmus MC Cancer Institute, Rotterdam, The Netherlands

[8]Oncode Institute, Utrecht, The Netherlands

Correspondence
Kazuhisa Chonabayashi, Department of Hematology and Oncology, Graduate School of Medicine, Kyoto University, 54 Kawahara-cho, Shogoin, Sakyo-ku, Kyoto 606-8507, Japan.
Email: kchona@kuhp.kyoto-u.ac.jp

Yoshinori Yoshida, Department of Cell Growth and Differentiation, Center for iPS Cell Research and Application, Kyoto University, 53 Kawahara-cho, Shogoin, Sakyo-ku, Kyoto 606-8507, Japan.
Email: yoshinor@cira.kyoto-u.ac.jp

Funding information
Japan Society for the Promotion of Science, Grant/Award Number: JP21K08414; Research Center Network for Realization of Regenerative Medicine (Japan Agency for Medical Research and Development), Grant/Award Number: JP20bm0104001 and JP20bm0804004; Acceleration Program of R&D and implementation for Regenerative Medicine and Cell and Gene Therapy (Japan Agency for Medical Research and Development), Grant/Award Number: JP23bm1323001 and JP23bm1423011; Project for Cancer Research and Therapeutic Evolution (Japan Agency for Medical Research and Development), Grant/Award Number: JP19cm0106235; Mochida Memorial Foundation for Medical and Pharmaceutical Research; Yasuda Memorial Medical Foundation; Kobayashi Foundation for Cancer Research; Daiichi Sankyo Foundation of Life Science; Fondation Leducq, Grant/Award Number: 18CVD05; iPS Cell Research Fund

Summary

Structural variations involving enhancer hijacking induce aberrant oncogene expression and cause tumorigenesis. A rare translocation, *t*(3;8)(q26.2;q24), is associated with *MECOM* and *MYC* rearrangement, causing myeloid neoplasms with a dismal prognosis. The most recent World Health Organization classification recognises myeloid neoplasms with *MECOM* rearrangement as acute myeloid leukaemia (AML) with defining genetic abnormalities. Recently, the increasing use of induced pluripotent stem cell (iPSC) technology has helped elucidate the pathogenic processes of haematological malignancies. However, its utility for investigating enhancer hijacking in myeloid neoplasms remains unclear. In this study, we generated iPSC lines from patients with myelodysplastic syndromes (MDS) harbouring *t*(3;8)(q26.2;q24) and differentiated them into haematopoietic progenitor cells to model the pathophysiology of MDS with *t*(3;8)(q26.2;q24). Our iPSC model reproduced the primary patient's *MECOM* expression changes and histone H3 lysine 27 acetylation (H3K27ac) patterns in the *MECOM* promoter and *MYC* blood enhancer cluster (BENC). Furthermore, we revealed the apoptotic effects of the bromodomain and extra-terminal motif (BET) inhibitor on iPSC-derived MDS cells by suppressing activated *MECOM*. Our study demonstrates the usefulness of iPSC models for uncovering the precise mechanism of enhancer hijacking due to chromosomal structural changes and discovering potential therapeutic drug candidates for cancer treatment.

KEYWORDS
BET inhibitor, enhancer hijacking, iPSC, MECOM, myeloid neoplasm

Momoko Nakamura and Kazuhisa Chonabayashi contributed equally to this work.

INTRODUCTION

Chromosomal structural variations may result in enhancer hijacking if an active enhancer is improperly positioned, causing it to regulate genes that are not its original targets.[1] This phenomenon has been described in some cancers, where an enhancer is relocated through chromosomal rearrangements to induce aberrant oncogene expression.[2] This has been revealed as the principal pathogenic mechanism in many haematological malignancies,[3,4] including myelodysplastic syndromes (MDS) and acute myeloid leukaemia (AML), which harbour recurrent chromosome 3 rearrangements, such as inv(3)(q21.3q26.2)/*t*(3;3)(q21.3;q26.2). Chromosomal rearrangements, such as inv(3)/*t*(3;3), juxtapose a *GATA2* distal haematopoietic enhancer with the *EVI1* promoter that causes aberrant EVI1 expression, which promotes proliferation and impairs the differentiation of myeloid precursor cells, leading to leukemogenesis.[5,6] Both MDS and AML with inv (3)/*t*(3;3) are associated with chemoresistance and have a 2-year survival rate lower than 10%.[7–9] A group of leukaemias with other 3q26/*MECOM* rearrangements, known as MDS/AML with atypical 3q26 rearrangements, often results in *MECOM* overexpression.[7,10] The rare translocation *t*(3;8)(q26.2;q24), an atypical 3q26/*MECOM* rearrangement, has been identified in a limited number of patients with myeloid neoplasms and is associated with *MECOM* and *MYC* rearrangement, resulting in poor prognosis with a median survival of 6 months.[11–14] Recent reports showed that atypical 3q26/*MECOM* rearrangements, including *t*(3;8)(q26.2;q24), also overexpress *MECOM* by repurposing enhancer elements from the translocation partners, similar to the enhancer hijacking of the *GATA2* distal enhancer in inv (3)/*t*(3;3).[11,12] Based on these findings, the World Health Organization (WHO) designated a new category of AML with *MECOM* rearrangement in 2022.[15] Many haematological malignancies involve enhancer hijacking,[16,17] and specific disease models need to be developed for novel drug discovery and development.

Induced pluripotent stem cells (iPSCs) were generated from somatic differentiated cells by Yamanaka and Takahashi.[18] Since their discovery, the application of iPSC technology has significantly contributed to our understanding of the pathophysiology of various inherited and acquired haematological disorders.[19,20] One of the key advantages of iPSCs in disease modelling is their comparability to isogenic controls, enabling the study of the cooperative effects of genomic alterations and their impact on disease progression via in vitro haematopoietic differentiation, colony-forming and replating assays and cell signalling studies. Another advantage of iPSCs is their ability to create complex, large-scale chromosomal rearrangements, such as translocations, which are difficult to achieve with genetic tools, such as clustered regularly interspaced short palindromic repeats (CRISPR). Moreover, disease modelling using iPSCs has consistently uncovered new therapeutic strategies.[21] Aberrant histone methylation and acetylation have been implicated in cancer development. In a previous report of iPSCs derived from AML patients with *KMT2A* translocations, reprogrammed AML-iPSCs reset their leukaemic DNA methylation profiles in the pluripotent state, thus effectively eliminating their leukaemic potential.[22] However, haematopoietic differentiation allowed the reacquisition of the leukaemic DNA methylation signature and phenotype, indicating that leukaemic genomic alterations associated with histone and DNA methylation are sufficient to induce leukemogenesis. To date, there are no reports on how aberrant histone acetylation in MDS/AML changes upon reprogramming into iPSCs or subsequent redifferentiation into haematopoietic cells.

In this study, we generated iPSC lines from a patient with MDS harbouring *t*(3;8)(q26.2;q24) and differentiated them into haematopoietic progenitor cells (HPCs) to model the pathophysiology of MDS with *t*(3;8)(q26.2;q24). Using this platform, we found that the bromodomain and extra-terminal motif (BET) inhibitor JQ1 suppressed *MECOM* expression and induced apoptosis in MDS cells carrying *t*(3;8)(q26.2;q24). Our study demonstrates the usefulness of iPSC models for uncovering the precise mechanism of enhancer hijacking due to chromosomal structural changes and discovering potential therapeutic drug candidates for cancer treatment.

MATERIALS AND METHODS

Generation of iPSCs from a patient with *t*(3;8)(q26.2;q24)

We established iPSCs from a patient with MDS carrying *t*(3;8)(q26.2;q24) using episomal vectors as previously described.[23] Briefly, bone marrow or peripheral blood mononuclear cells from the patient were transfected with an episomal vector mix, including pCXLE-hOCT3/4-shp53, pCXLE-hSK, pCXLE-hUL and pCXWB-EBNA1, and seeded onto mouse embryonic fibroblast feeder cells. Isogenic normal iPSCs were generated after T-cell activation using Dynabeads Human T-Activator CD3/CD28 (Thermo Fisher Scientific) according to the manufacturer's instructions. MDS-iPSC lines were denoted as MDS-25-A3, MDS-25-B8, MDS-25-G1, MDS-25-J1 and MDS-25-J4 iPSCs, and isogenic normal iPSC lines were denoted as N-25-A1 and N-25-B1 iPSCs. We also used an iPSC line derived from a healthy donor (692D2) as a control. Chromosomal G-band analysis of the iPSC lines was performed at Nihon Gene Research Laboratories (Sendai, Japan). This study was approved by the Ethics Committees of the Graduate School of Medicine, Kyoto University and Kyoto University Hospital and performed according to the Declaration of Helsinki. Written informed consent was obtained from the patient.

Statistical analyses

GraphPad Prism 10 (GraphPad Software) was utilised to conduct all statistical analyses. $p < 0.05$ was considered statistically significant.

RESULTS

Translocation of 8q24/*MYC* to 3q26/*MECOM* causes aberrant *MECOM* expression in a patient with MDS harbouring *t*(3;8)(q26.2;q24)

We identified a patient with atypical 3q26/*MECOM*-rearranged MDS who succumbed to the disease within 5 months of diagnosis (Table 1). Bone marrow aspiration revealed a blast cell percentage of 19.6% (Figure 1A). Immunostaining of the bone marrow clot demonstrated high MECOM and low MYC expression (Figure 1B,C). Karyotype analysis revealed a translocation between chromosomes 3 and 8 (46, XY, *t*(3;8)(q26.2;q24), del (9)(q?)) (Figure 1D). Fluorescence in situ hybridisation analysis indicated that over 90% of the split signals for *MECOM* and *c-MYC* were positive (Figure S1). Targeted sequencing identified mutations in *ETNK1* (p.N155S), *PTPN11* (p.D61V, p.A72T, and p.E76K), and *EZH2* (c.2181-1G>C) (Table S1). Copy number alteration confirmed a decrease in the total copy number on chromosome 9 and abnormalities in the allelic ratio on chromosomes 7 and 9 due to the deletion of chromosome 9 and uniparental disomy on chromosome 7 (Figure S2A). Whole-genome sequencing revealed that the breakpoints were 6.4 kb upstream of *MECOM* (6.4 kb upstream of the *MDS1-EVI1* promoter and 523 kb upstream of the *EVI1* promoter) and 200 kb upstream of blood enhancer cluster (BENC), which is known as the *MYC* super-enhancer (Figure 1E; Figure S2B–D). This specific breakpoint location is consistent with those in previously reported cases of *t*(3;8) MDS/AML.[11,12] These findings suggest that the *t*(3;8)(q26.2;q24) translocation may be causally associated with the high *MECOM* expression and MDS development in this patient.

Generation of MDS-iPSC and isogenic normal iPSC lines from the patient with MDS harbouring *t*(3;8)(q26.2;q24)

We generated several iPSC lines derived from MDS clones and two iPSC lines derived from normal T cells of a patient with *t*(3;8)(q26.2;q24) (Figure 1F; Figure S3A; Table S2). Karyotype analysis of MDS-iPSC lines revealed concordance with the patient karyotype (Figure 1F; Figure S3B–D). Conversely, isogenic normal iPSC lines exhibited normal karyotypes (Figure 1F; Figure S3E,F). Sanger sequencing showed that the MDS-iPSC lines had the same breakpoint as the patient (Figure S3G; Table S3). Gene expression of pluripotency markers, including *NANOG*, *OCT3/4* and *SOX2*, was verified using quantitative RT-PCR (Figure S3H; Table S4). The MDS-iPSC lines displayed a characteristic morphology and expressed pluripotent stem cell markers at levels comparable to those of the isogenic normal iPSC lines (Figure S3I). The mutations present in the starting bone marrow samples were assessed through Sanger sequencing of five generated MDS-iPSC lines, revealing *ETNK1* and *EZH2* mutations in all lines, with only one line harbouring the *PTPN11* (p.A72T) mutation (Figure 1F; Tables S3 and S5). By contrast, the two isogenic normal iPSC lines revealed no mutations present in the patient (Figure 1F; Tables S3 and S5). These findings demonstrated that MDS cells were successfully reprogrammed into iPSCs, retaining the original genomic abnormalities.

MDS-iPSCs exhibited reduced haematopoietic potential and decreased clonogenic capacity

Next, we differentiated MDS-iPSC, isogenic normal iPSC and control iPSC lines into haematopoietic cells via embryoid body formation (Figure 2A). MDS-iPSC lines gave rise to $CD45^+$ haematopoietic cells with efficiencies comparable to those of isogenic normal iPSC lines but retained CD34 expression until day 17 and beyond (Figure 2B). In addition, the MDS-iPSC lines did not produce $CD235a^+$ erythroid cells (Figure 2C). Haematopoietic cells derived from MDS-iPSCs express the myeloid lineage marker CD33, which is known to be highly expressed in AML blasts (Figure S4). FACS-sorted $CD45^+CD34^+$ HPCs from MDS-iPSC lines demonstrated leukaemic blast morphology (Figure 2D) and showed markedly decreased myeloid

TABLE 1 Clinical and haematological characteristics.

		Peripheral blood findings				Bone marrow findings		Treatment and follow-up		
Age	Sex	WBC, $\times 10^9$/L	Hb, g/dL	Plt, $\times 10^9$/L	Blast, %	Blast, %	Dysplasia	Treatment	Survival, months	Outcome
72	M	9.63	5.1	322	10	19.6	Yes (MKs)	5-Azacitidine	5	Dead

Abbreviations: Hb, haemoglobin; MKs, megakaryocytes; Plt, platelet; RBC, red blood cell; WBC, white blood cell.

FIGURE 1 Translocation of 8q24/*MYC* to 3q26/*MECOM* causes aberrant *MECOM* expression in a patient with MDS carrying *t*(3;8)(q26.2;q24). (A) Morphology of bone marrow cells. May Grünwald–Giemsa staining revealed blast cells with large nuclei, scant cytoplasm and no cytoplasmic granules. Magnification of the objective lens was 40×. Scale bar, 50 μm. (B, C) Immunostaining of bone marrow clots of MECOM (B) and MYC (C). Magnification of the objective lens was 40×. Scale bar, 50 μm. (D) Karyotype analysis of bone marrow cells. (E) Schematic diagram of whole-genome sequencing results for the MDS clones. This figure was created using BioRender.com. (F) Schematic representation of iPSC generation from blood cells of a patient with *t*(3;8)(q26.2;q24) and genetic information of the iPSC lines. The top panels show all recurrent gene mutations and chromosomal abnormalities detected in the starting cells used for reprogramming and their frequency. The bottom panels present the individual iPSC lines corresponding to their genetic profile. The MDS-iPSC lines were denoted as MDS-25-A3, MDS-25-B8, MDS-25-G1, MDS-25-J1 and MDS-25-J4 iPSCs, and the isogenic normal iPSC lines as N-25-A1 and N-25-B1 iPSCs. VAF, variant allele frequency. The figure was created using BioRender.com.

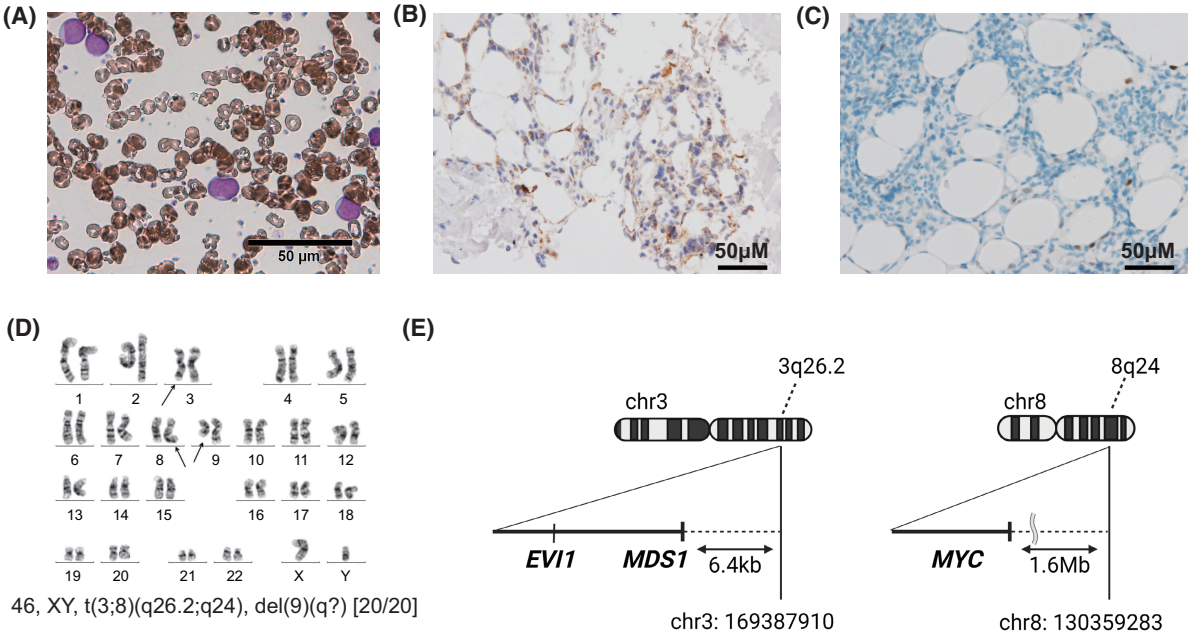

(F)

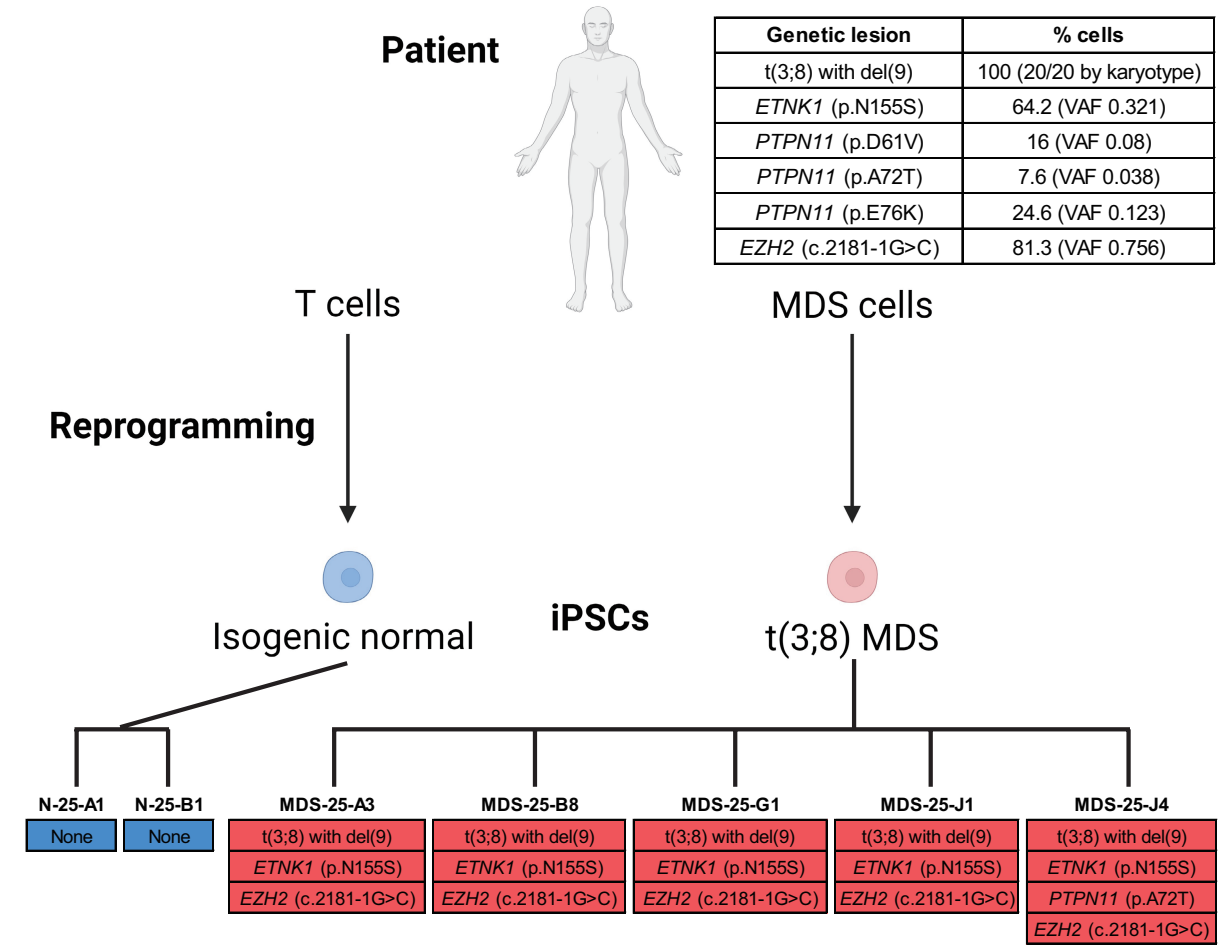

Genetic lesion	% cells
t(3;8) with del(9)	100 (20/20 by karyotype)
ETNK1 (p.N155S)	64.2 (VAF 0.321)
PTPN11 (p.D61V)	16 (VAF 0.08)
PTPN11 (p.A72T)	7.6 (VAF 0.038)
PTPN11 (p.E76K)	24.6 (VAF 0.123)
EZH2 (c.2181-1G>C)	81.3 (VAF 0.756)

colony-forming ability with no erythroid potential in contrast to those from the control and isogenic normal iPSC lines (Figure 2E,F). These results demonstrated that MDS-iPSC-derived HPCs had differentiation defects in both the myeloid and erythroid lineages.

MDS-iPSC-derived HPCs exhibited an aberrant gene expression pattern similar to that of primary myeloid neoplasm cells

Next, we performed RNA sequencing (RNA-seq) on $CD45^+CD34^+$ HPCs derived from MDS-iPSCs and isogenic normal iPSCs (Figure 3A). Principal component analysis revealed that MDS-iPSCs were located on the positive side of principal component 1, accounting for 97% of the variance, whereas those derived from isogenic normal iPSCs were located on the negative side (Figure 3B). We compared the differentially expressed genes in MDS-25-G1 and N-25-A1 iPSC-derived HPCs and created a volcano plot, revealing the significant downregulation of 726 genes in MDS-25-G1 iPSC-derived HPCs, including critical factors expressed during haematopoietic differentiation, and the significant upregulation of 2018 genes in MDS-25-G1 iPSC-derived HPCs, including factors with previously described functions in haematopoietic stem cell (HSC) maintenance (Figure 3C).[24] Gene set enrichment analysis showed enrichment of gene expression signatures of primary AML cells in HPCs derived from MDS-iPSCs (Figure 3D,E; Table S6). These transcriptome data support the myeloid neoplasm phenotype of MDS-iPSC-derived HPCs.

MDS-iPSC-derived HPCs showed high *MECOM* expression comparable to that in original MDS cells

We compared *MECOM* expression among iPSCs, iPSC-derived HPCs, K562 cells, and $CD34^+$ HPCs from the patient. Gene expression analysis of the *MDS1-EVI1* variant and total *MECOM* was performed using qRT-PCR with primers listed in Table S4. Haematopoietic differentiation of iPSCs into HPCs increased *MECOM* expression (Figure 4A,B; Figure S5A,B). MDS-iPSC-derived HPCs showed higher expression of the *MDS1-EVI1* variant and total *MECOM* than isogenic normal iPSC-derived HPCs. *MECOM* expression levels in MDS-iPSC-derived HPCs were comparable to those in HPCs from the patient (Figure 4C,D). Consistent with a previous report,[12] *MYC* expression in MDS-iPSC-derived HPCs was not significantly different from that in isogenic normal iPSC-derived HPCs (Figure 4E; Table S4). These results suggest that the translocation caused high *MECOM* expression, especially of the *MDS1-EVI1* variant, which may be involved in MDS pathogenesis in this patient.

MECOM promoter hyperactivation upon interaction with *MYC* super-enhancer in *t*(3;8) MDS

We conducted H3K27ac ChIP sequencing (ChIP-seq) with iPSCs, iPSC-derived $CD45^+CD34^+$ HPCs, K562 cells and $CD34^+$ HPCs from the patient according to previous reports (Tables S7 and S8).[12,25] ChIP-seq revealed BENC activity in both control iPSC- and MDS-iPSC-derived HPCs in a pattern similar to that of the patient $CD34^+$ HPCs (Figure 5A). BENC is a cluster of multiple individual enhancer modules (A–I), which encompasses approximately 150 kb of chromatin enriched with the histone mark H3K27ac and is located 1.7 Mb downstream of *MYC*. This locus has been documented as essential for normal haematopoiesis.[25] H3K27ac levels, as determined via ChIP-seq, revealed both *MDS1-EVI1* and *EVI1* promoter activity in control iPSC- and MDS-iPSC-derived HPCs, and the patient HPCs (Figure 5B; Figure S6A–D). However, *MDS1-EVI1* promoter activity was higher in MDS-iPSC-derived HPCs and patient primary HPCs than in control iPSC-derived HPCs, consistent with the markedly increased expression of the *MDS1-EVI1* variant in these MDS samples (Figure 4A). These data support the hypothesis that *MECOM* overexpression in this patient with *t*(3;8) MDS results from translocation of the *MYC* super-enhancer.

t(3;8) MDS cells exhibited H3K27 acetylation in the *MDS1-EVI1* promoter region after reprogramming

To evaluate the effects of cell reprogramming and differentiation on histone modification, we compared H3K27ac activation between iPSCs and iPSC-derived HPCs. Initially, we examined the activity of genes specific to each cell type and made intriguing discoveries. Specifically, we observed the unique activation of *NANOG*, *POU5F1* (*OCT3/4*) and *SOX2* in iPSCs (Figure S7A–C). By contrast, the *EVI1* promoter and *GATA2* enhancer exhibited activity only in iPSC-derived HPCs (Figure 5B; Figures S6A,B and S7D). Unexpectedly, active H3K27ac in the *MDS1-EVI1* promoter region was detected at low levels in MDS-iPSCs as well as in iPSC-derived HPCs (Figure 5B; Figure S6C,D). This result was consistent with the higher *MDS1-EVI1* expression in MDS-iPSCs than in control iPSCs (Figure 4A; Figure S5A).

Bromodomain-containing 4 (BRD4) inhibitor JQ1 suppressed *MECOM* expression and *t*(3;8) MDS cell growth

BRD4 is a member of the BET subfamily that abundantly accumulates at super-enhancers.[26] BRD4 inhibitors, such

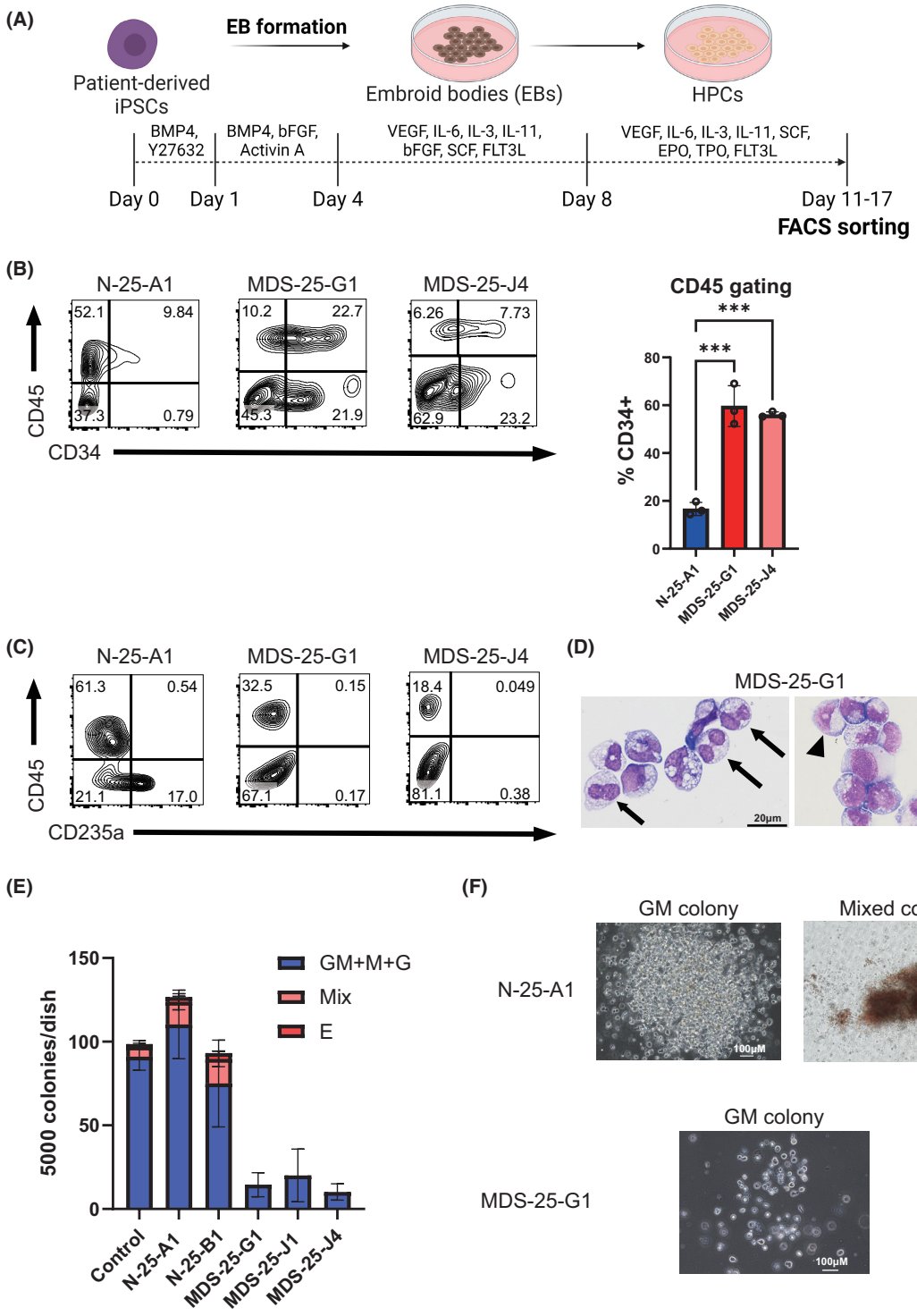

FIGURE 2 MDS-iPSCs exhibit reduced haematopoietic potential and decreased clonogenic capacity. (A) Schema of a protocol for the haematopoietic differentiation from iPSCs. The images were created using BioRender.com. (B) Representative flow cytometry data in the N-25-A1, MDS-25-G1 and MDS-25-J4 iPSC lines on day 17. Percentages of $CD34^+$ HPCs in $CD45^+$ cells with the N-25-A1, MDS-25-G1 and MDS-25-J4 are shown in the right-hand graph. The results of three independent experiments are shown. (C) Representative flow cytometry data of $CD235a^+$ cells in the N-25-A1, MDS-25-G1 and MDS-25-J4 iPSC lines on day 17. (D) May Grünwald–Giemsa staining of $CD45^+$ (left) and $CD45^+CD34^+$ (right) haematopoietic cells derived from the MDS-25-G1 iPSC lines. Dysplastic changes (arrow point to pseudo Pelger–Huet cells) and leukaemic blast morphology (arrowhead) are observed. Magnification of the objective lens was 100×. Scale bar, 20 μm. (E) Haematopoietic colony formation assay of HPCs derived from one control iPSC, two isogenic normal iPSC (N-25-A1 and N-25-B1) and three MDS-iPSC (MDS-25-G1, MDS-25-J1 and MDS-25-J4) lines. Each line was tested in three independent experiments. (F) Representative images of GM (top left) and mixed (top right) colonies derived from the N-25-A1 line and GM (bottom) colonies derived from the MDS-25-G1 line. Magnification of the objective lens: 10×. Scale bar, 100 μm. *p*-values were calculated using a one-way analysis of variance with Dunnett's correction. ***$p < 0.001$. Data are presented as means ± SD.

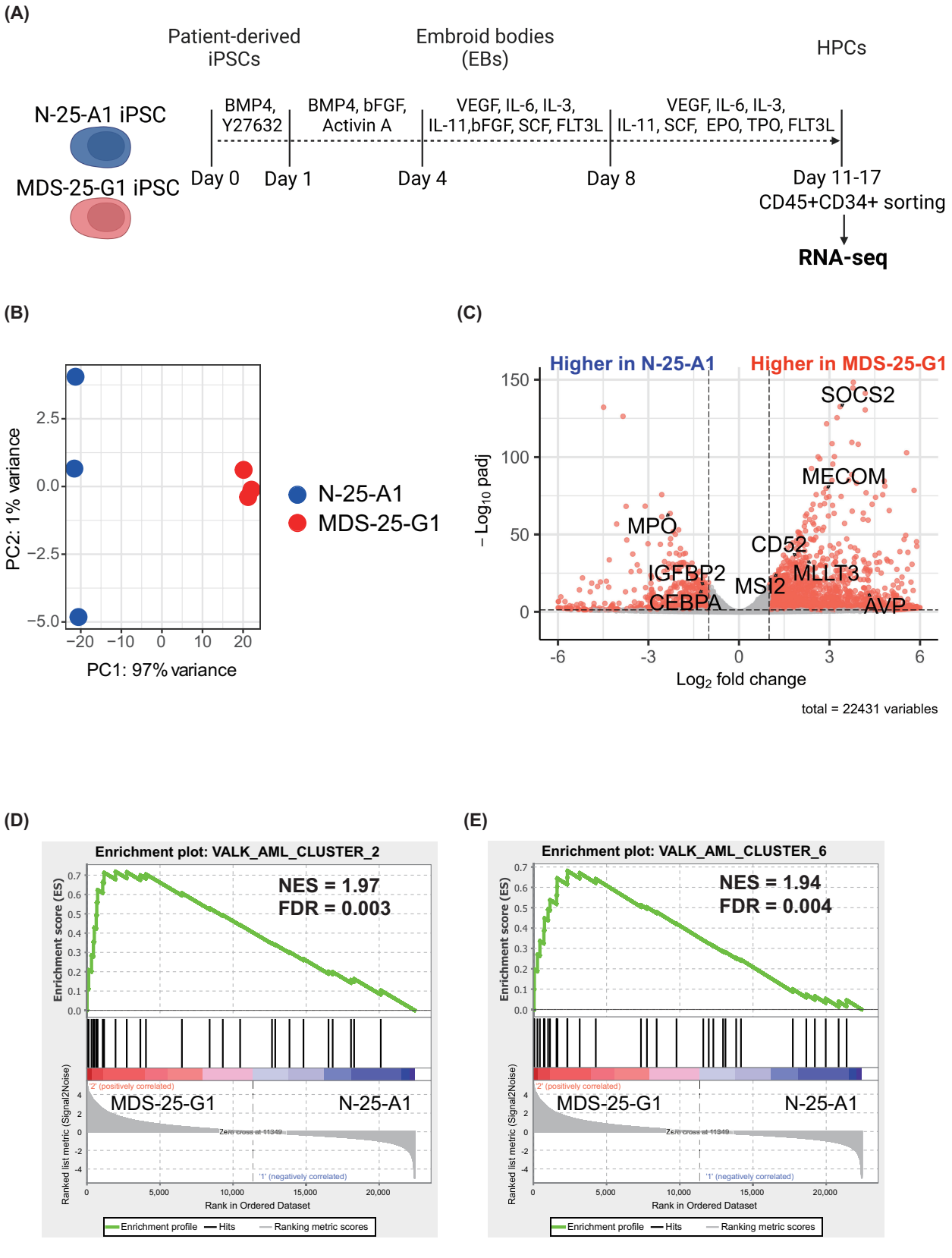

FIGURE 3 MDS-iPSC-derived HPCs exhibit an aberrant gene expression pattern similar to that of primary myeloid neoplasm cells. (A) The protocol scheme for the haematopoietic differentiation from iPSCs and an RNA-seq sample collection time point. The image was created using BioRender.com. (B) Principal component analysis of HPCs derived from the N-25-A1 and the MDS-25-G1 lines with RNA-seq. (C) Volcano plot presenting the differential gene expression between HPCs derived from the N-25-A1 and MDS-25-G1 lines. Each dot indicates one gene; red dots represent $\log_2$ fold change (log2FC) of >1 or −1.0 and adjusted *p*-value (padj) <0.05. (D, E) Gene set enrichment analysis of the VALK_AML_CLUSTER_2 (D) and the VALK_AML_CLUSTER_6 (E) data sets showed enrichment of MDS-25-G1 iPSC-derived HPCs.

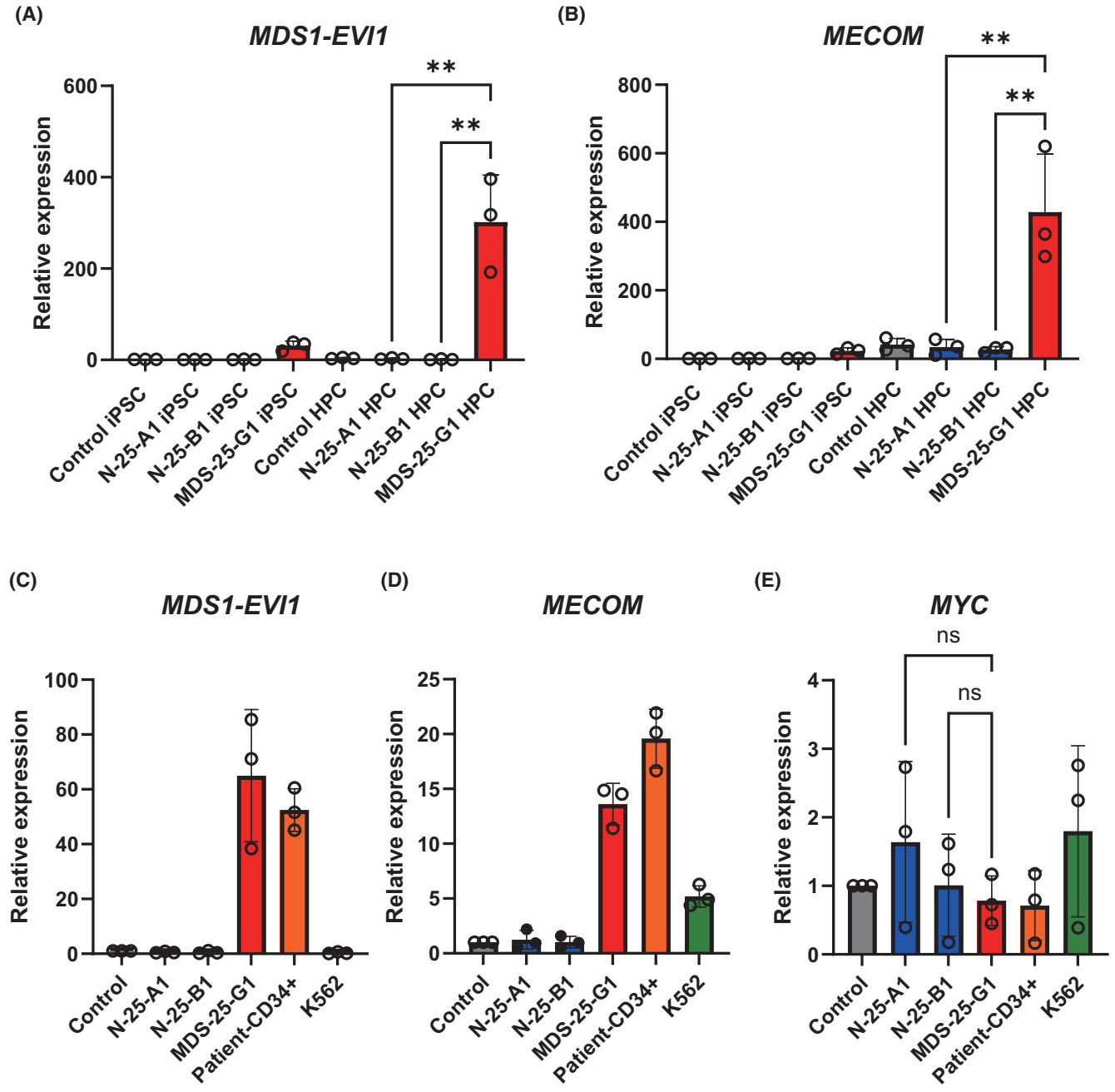

FIGURE 4 HPCs derived from MDS-iPSCs show higher *MECOM* expression levels, comparable to those in MDS cells from the patient. (A, B) Expression levels of *MDS1-EVI1* (A) and *MECOM* (B) in iPSCs and HPCs derived from one control iPSC line, two isogenic normal iPSC lines and one MDS-iPSC line. Each line was tested in three independent experiments. Expression levels were normalised to the level of *GAPDH*. (C–E) Expression levels of *MDS1-EVI1, MECOM* and *MYC* in HPCs derived from control iPSC, N-25-A1, N-25-B1 and MDS-25-G1 lines, $CD34^+$ HPCs from the patient and K562. The results of three independent experiments are shown. Expression levels were normalised to the level of *GAPDH*. *p*-values were calculated using a one-way analysis of variance with Dunnett's correction. $^{**}p < 0.01$; ns, not significant. Data are presented as means ± SD.

as JQ1, inhibit the function of super-enhancers, leading to the selective repression of oncogenes in haematological malignancies.[17,27] Since the BENC super-enhancer appeared to promote *t*(3;8) MDS development by activating *MECOM* expression, we examined whether JQ1 abrogated the proliferation of MDS-iPSC-derived HPCs in vitro. As expected, JQ1-treated MDS-iPSC-derived HPCs had significantly lower expression levels of *MECOM* than DMSO-treated HPCs (Figure 6A,B). Conversely, control iPSC-derived HPCs did not differ significantly in *MECOM* expression between the JQ1-treated and untreated groups (Figure S8A,B). Next, we assessed JQ1-induced apoptosis using Annexin V/7-AAD staining and flow cytometry. JQ1 markedly increased the fraction of apoptotic cells in a dose-dependent manner in MDS-iPSC-derived HPCs, but not in control and N-25-A1 iPSC-derived HPCs and K562 cell lines (Figure 6C,D; Figure S8C). Using a trypan blue exclusion assay, we also assessed cell viability after

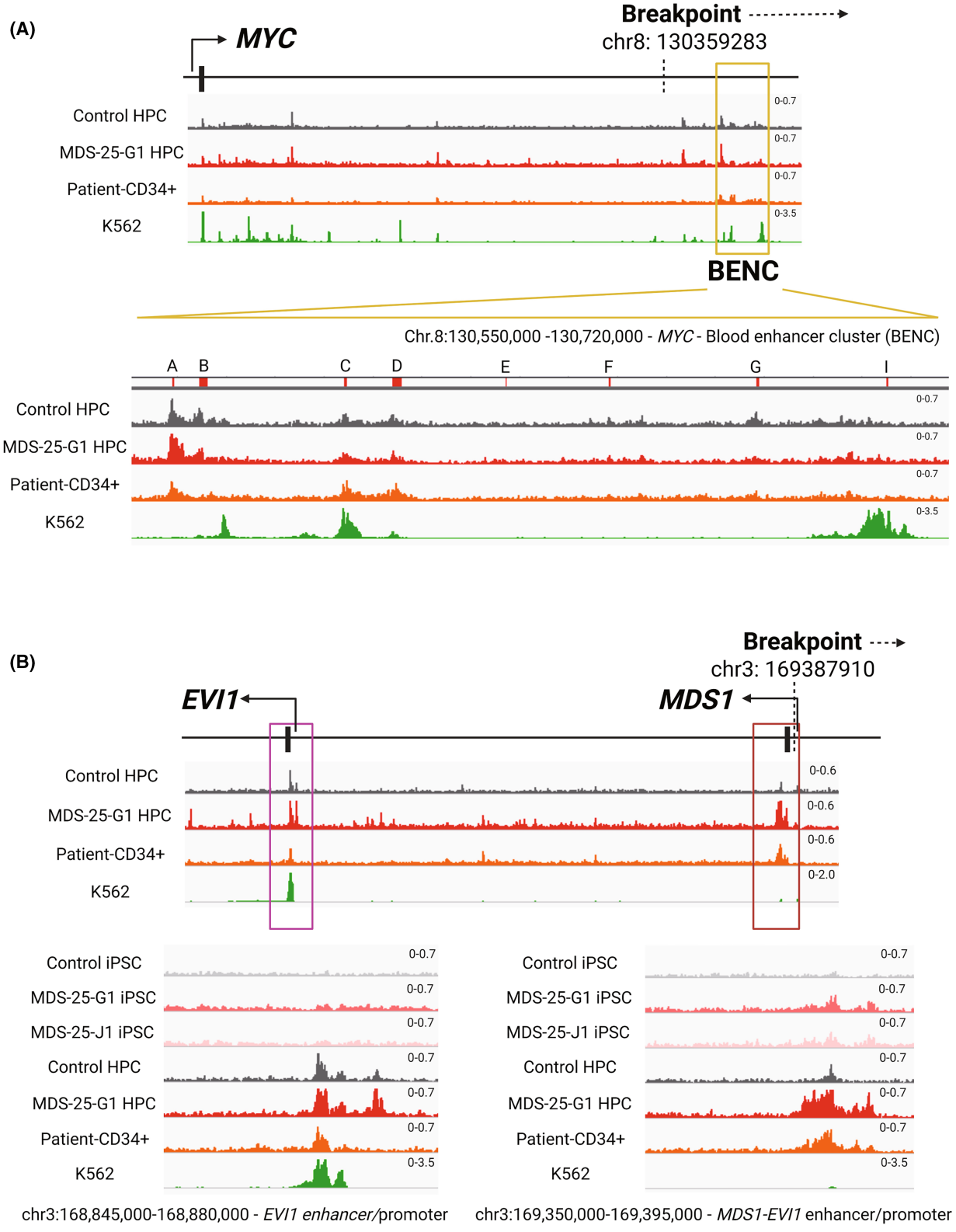

FIGURE 5 *MECOM* promoter hyperactivation upon interaction with *MYC* super-enhancer in *t*(3;8) MDS. (A) Upper part: Presenting chr8q24, H3K27ac ChIP-seq data for HPCs derived from control iPSC (grey) and MDS-iPSC (red, MDS-25-G1) lines, $CD34^+$ HPCs (orange) from the patient and K562 (green). A chromosome 8 breakpoint in the patient with *t*(3;8)(q26.2;q24). Lower part: H3K27ac ChIP-seq data as in the upper part but presenting a close-up of the +1.7 Mb *MYC* super-enhancer (BENC) with previously characterised individual enhancer modules A–I.[25] (B) Upper part: Similar to (A) but close-up of the *MECOM* gene. A chromosome 3 breakpoint in the patient with *t*(3;8)(q26.2;q24). Lower left part: H3K27ac ChIP-seq data for control iPSCs (light grey), MDS-25-G1 iPSCs (light red), MDS-25-J1 iPSCs (pink), HPCs derived from control iPSC (grey), MDS-25-G1 iPSC (red) lines, $CD34^+$HPCs (orange) from the patient and K562 (green) at the *EVI1* locus. The peak located at the *EVI1* transcriptional start site marks the promoter region. Lower right part: Similar to the left part but comparing *MDS1* promoter activation. These schemas were created using BioRender.com.

JQ1 treatment. We found that HPCs derived from MDS-25-G1 iPSC showed a more significant decrease in viability than HPCs derived from the control and N-25-A1 lines (Figure 6E,F; Figure S8D). This cytotoxic effect was also observed in HPCs derived from other MDS-iPSC clones and $CD34^+$ MDS cells from the patient after JQ1 treatment (Figure S9A,B). Furthermore, we confirmed the effect of JQ1 in the EVI1-GFP *t*(3;8) K562 cell line model reported previously.[12] JQ1 administration resulted in a modest reduction in the degree of GFP expression within *t*(3;8) K562 cells (Figure 6G). Additionally, H3K27ac ChIP sequencing revealed a reduction in the level of H3K27ac modifications in BENC after JQ1 treatment (Figure 6H; Figure S9C). These results suggest that JQ1 inhibition of the BENC super-enhancer impairs the growth of *t*(3;8) MDS cells by suppressing aberrantly activated *MECOM* (Figure 7).

DISCUSSION

Myeloid neoplasms with *t*(3;8)(q26.2;q24), which often leads to *MECOM* and *MYC* rearrangement, have an extremely poor prognosis with a median survival of 6 months.[13] Myeloid neoplasms with atypical 3q26 rearrangements, including *t*(3;8)(q26.2;q24), share some similarities with myeloid neoplasms associated with inv (3)/*t*(3;3).[11,12] The WHO 2022 classification recognises these myeloid neoplasms with 3q26 rearrangements as AML with defining genetic abnormalities.[15]

The expression of both *EVI1* and *MDS1-EVI1* was aberrantly upregulated in our patient with MDS *t*(3;8)(q26.2;q24). *MECOM* translocation reportedly leads to *EVI1* overexpression without upregulating *MDS1-EVI1* in most cases of atypical 3q26-rearranged AML.[11] The chromosomal breakpoints identified in this study occur commonly between *MDS1* and *EVI1* or downstream of *EVI1*.[5,11] Lugthart et al.[7] reported positive *MDS1-EVI1* expression in 50% of inv(3)/*t*(3;3) cases and 57% of the *t*(3q26) group. Hence, *MDS1-EVI1* expression appears to be influenced by the breakpoint location. In our case, the breakpoint *t*(3;8)(q26.2;q24) was located immediately upstream of the *MDS1* promoter, resulting in high *MDS1-EVI1* expression.

To date, patient-derived iPSC models have helped elucidate the pathogenic process of many human diseases, including myeloid neoplasms, and serve as a valuable drug discovery platform.[28–31] Our iPSC model of atypical 3q26-rearranged MDS reproduced the *MECOM* expression changes and H3K27ac patterns in the primary patient. A previous study has reported that leukaemic DNA methylation and gene expression profiles were reset after reprogramming, but the leukaemic properties were reactivated upon haematopoietic differentiation.[22] The current study demonstrates that *MECOM* expression and H3K27ac activation of the *MECOM* promoter and the *MYC* distal enhancer increased after haematopoietic differentiation. However, MDS-iPSCs with *t*(3;8)(q26.2;q24) exhibited H3K27ac activation at the *MECOM* promoter, even in the pluripotent state, with higher *MECOM* expression than the control iPSCs. One possibility is that these abnormal histone marks are maintained during MDS cell reprogramming to iPSCs. Alternatively, histone acetylation at the *MECOM* promoter of MDS cells could be reset following reprogramming and acquire aberrant histone activation soon after reprogramming owing to the influence of the translocation.

The BET inhibitor JQ1 has demonstrated activity against MDS/AML cells with inv(3)/*t*(3;3) through epigenetic silencing of the translocated *GATA2* enhancer.[5] We speculated that repressing super-enhancer-dependent *MECOM* expression could also induce cytotoxicity to MDS/AML clones with atypical 3q26 rearrangement. The previous study reported that the deletion of the *MYC* distal enhancer resulted in the loss of *MECOM* expression. Our data, along with the recent report, support the hypothesis that *MECOM* overexpression in myeloid neoplasms with *t*(3;8) is driven by the translocation of the *MYC* distal enhancer.[12] This study provides the first proof of concept that aberrant *MECOM* expression in MDS/AML cells with *t*(3;8)(q26.2;q24) can be suppressed by BET inhibitors, indicating that iPSCs are valuable tools for uncovering the mechanisms and treatment of enhancer hijacking.

Despite the promising results, our iPSC model has certain limitations. First, the patient with MDS carried a chromosome 9 deletion along with the translocation of *t*(3;8)(q26.2;q24) and some recurrent gene mutations related to MDS/AML. These abnormalities could also affect gene expression and disease phenotypes, implying that we did not completely assess the function of *t*(3;8)(q26.2;q24). Second, the HPCs differentiated from iPSCs do not fully resemble bona fide HSCs with long-term repopulation. Despite these limitations, we modelled enhancer hijacking events in cancers using iPSCs for the first time. This patient-specific iPSC platform may be helpful in precise epigenetic analysis and functional studies of cancers associated with enhancer hijacking, such as myeloid neoplasms with *t*(3;8)(q26.2;q24).

In conclusion, this study provided novel biological and therapeutic insights into myeloid neoplasms with *t*(3;8)(q26.2;q24). Using patient-derived iPSCs, we demonstrated that *MYC* distal enhancer translocation and the consequent increase in *MECOM* promoter activity contribute to the abnormal maturation of HPCs and oncogenic processes. Furthermore, we revealed the apoptotic effects of the BET inhibitor JQ1 on MDS cells harbouring *t*(3;8)(q26.2;q24) by suppressing aberrantly activated *MECOM*. Our results demonstrate the efficacy of iPSC models in elucidating the mechanism of enhancer hijacking resulting from alterations in chromosomal structure and in identifying prospective therapeutic agents for cancer treatment.

AUTHOR CONTRIBUTIONS

M.Nakamura., K.C. and Y.Y. conceived and designed the research; M.Nakamura performed most of the experiments, analysed the data and wrote the manuscript; K.C. established MDS-iPSC lines and performed some experiments,

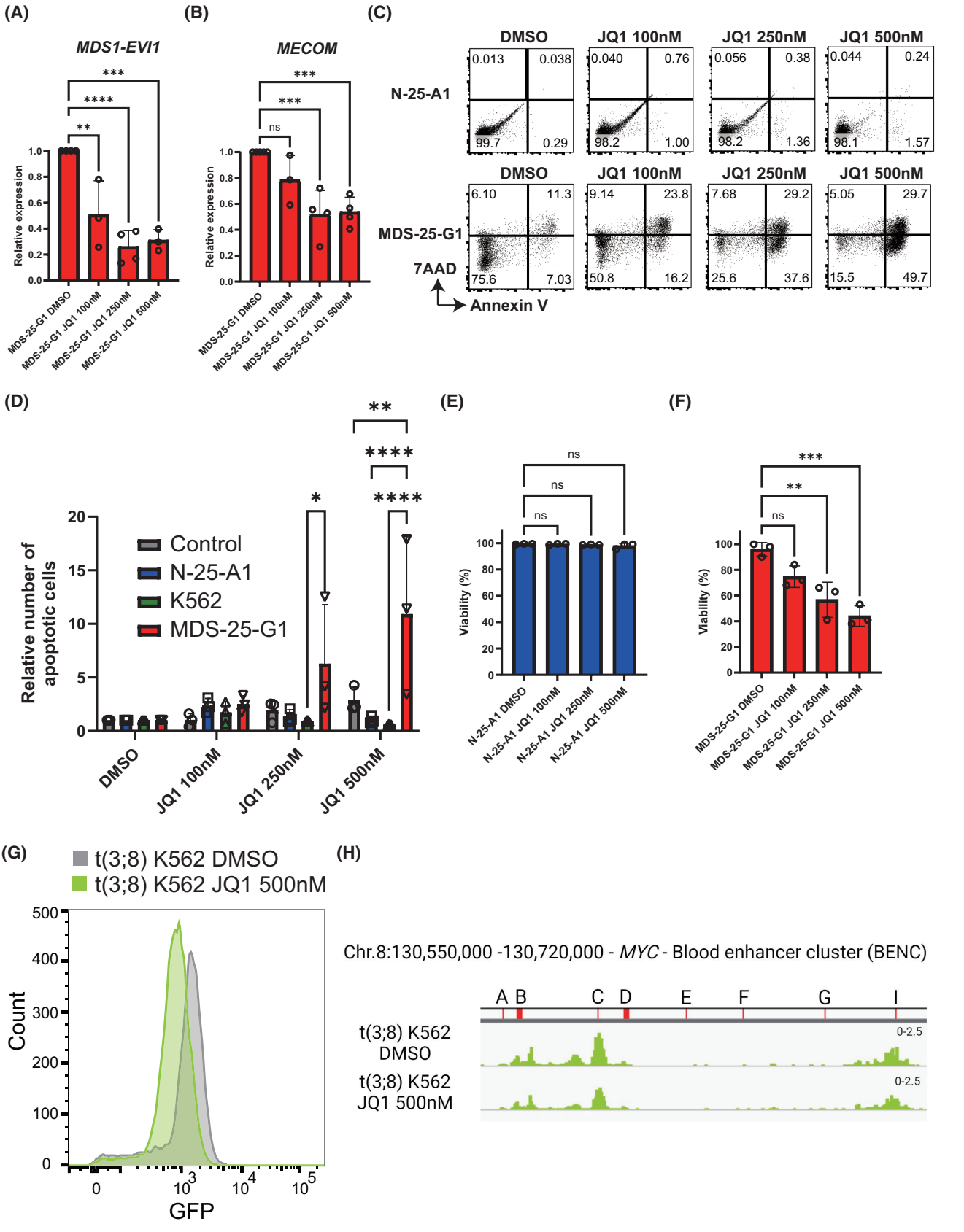

analysed the data and wrote the manuscript; M.Narita, Y.M. and M.Nishikawa provided essential experimental support; Y.O. assisted with the ChIP-seq; M.H. collected patient blood samples and advised on the experimental design; Y.N. performed targeted capture sequencing and whole-genome sequencing; D.I., R.D., S.O. and A.T.-K. advised on the experimental design and wrote the manuscript; Y.Y. supervised the overall research and wrote the manuscript. All

FIGURE 6 JQ1 suppresses aberrant *MECOM* expression and induces apoptosis in *t*(3;8) MDS cells. (A, B) Expression levels of *MDS1-EVI1* (A) and *MECOM* (B) in HPCs derived from MDS-iPSCs (MDS-25-G1) after JQ1 treatment. The results of three or more independent experiments are shown. Expression levels were normalised to the level of *GAPDH*. (C) Assessment of apoptosis in HPCs derived from N-25-A1 (top) and MDS-25-G1 (bottom) iPSC lines after JQ1 treatment. Representative flow cytometry plots for Annexin V and 7-AAD staining with percentages for each gate are shown. (D) Relative number of Annexin V-positive cells in HPCs derived from control iPSC (grey), N-25-A1 (blue), K562 (green) and MDS-25-G1 (red) lines after JQ1 treatment. The cell number of Annexin V-positive cells in each DMSO-treated cell line was set to 1. (E, F) Cell viability in HPCs derived from N-25-A1 (E) and MDS-25-G1 (F) lines after JQ1 treatment, assessed by trypan blue exclusion assay. (G) Flow cytometry data of GFP expression in the EVI1-GFP *t*(3;8) K562 model 3 days after 500 nM JQ1 treatment. (H) H3K27ac-ChIP sequencing data post-JQ1 treatment in *t*(3;8) K562 cells on the +1.7 Mb *MYC* super-enhancer (BENC). *p*-values were calculated using a one-way analysis of variance with Dunnett's correction and a two-way analysis of variance with Tukey's correction. $*p<0.05$; $**p<0.01$; $***p<0.001$; $****p<0.0001$; ns, not significant. DMSO, dimethyl sulphoxide. Data are presented as means ± SD.

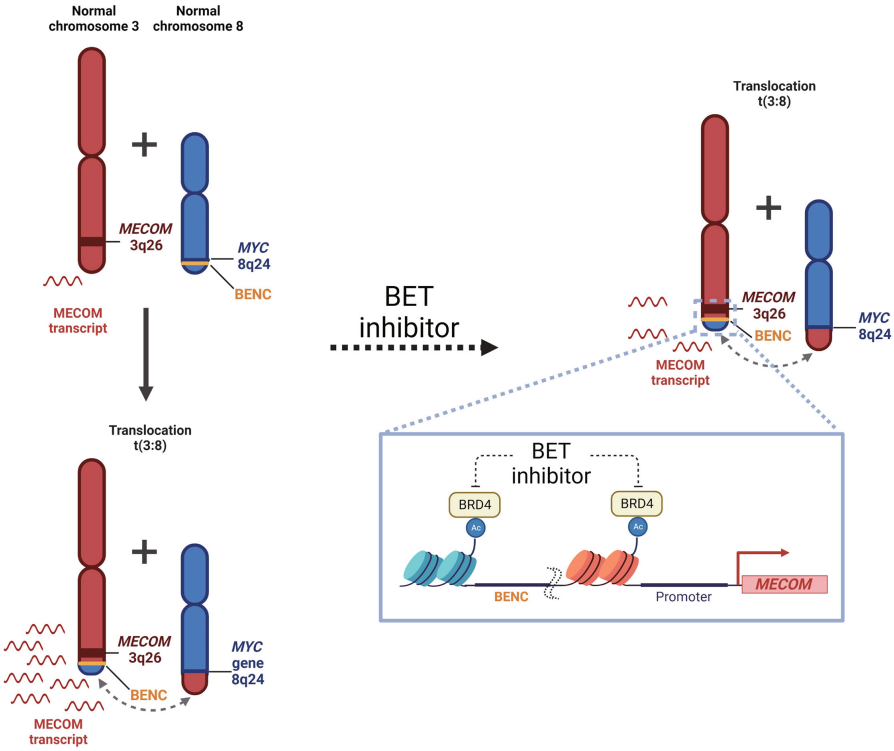

FIGURE 7 Schematic representation of the results. *MECOM* overexpression is driven by enhancer hijacking caused by the translocation *t*(3;8)(q26.2;q24), involving a super-enhancer (BENC). Administration of the BET inhibitor JQ1 suppressed super-enhancer activity and abrogated the aberrant expression of *MECOM*. The figure was created using BioRender.com.

authors interpreted the data and reviewed and approved the final manuscript.

ACKNOWLEDGEMENTS

We are grateful to Kelvin Hui for proofreading the manuscript. We would like to thank Editage (www.editage.com) for English editing. In preparing this work, ChatGPT was used to proofread the manuscript.

FUNDING INFORMATION

This work was supported in part by grants from JSPS KAKENHI (JP21K08414 (K.C.)), the Research Center Network for Realization of Regenerative Medicine (JP20bm0104001 (Y.Y.), JP20bm0804004 (K.C. and Y.Y.)), the Acceleration Program of R&D and implementation for Regenerative Medicine and Cell and Gene Therapy (JP23bm1423011 and JP23bm132300) and the Project for Cancer Research and Therapeutic Evolution (JP19cm0106235 (Y.Y. and K.C.)) provided by the Japan Agency for Medical Research and Development, grants from the Mochida Memorial Foundation for Medical and Pharmaceutical Research (Y.Y. and K.C.), a grant from Yasuda Memorial Medical Foundation (Y.Y.), grants from the Kobayashi Foundation for Cancer Research (K.C. and Y.Y.), a grant from the Daiichi Sankyo Foundation of Life Science (Y.Y.), a grant from the Leducq Foundation (18CVD05 (Y.Y.)) and the iPS Cell Research Fund (Y.Y.).

CONFLICT OF INTEREST STATEMENT

Y.Y. is a scientific advisor of Orizuru Therapeutics and receives grants from Astellas Pharma Inc, Takeda Pharmaceutical Company, Rohto, Toagosei, and Altos Labs, Inc outside the submitted work. D.I. receives grants from AbbVie and Sumitomo Pharma outside the submitted work.

DATA AVAILABILITY STATEMENT

ChIP-seq data are available from GEO under accession number GSE248238. RNA-seq data are available from GEO under accession number GSE248239. For the original data, please e-mail the corresponding authors.

ETHICS APPROVAL STATEMENT

This study was approved by the Ethics Committees of the Graduate School of Medicine, Kyoto University and Kyoto University Hospital and performed according to the Declaration of Helsinki.

PATIENT CONSENT STATEMENT

Written informed consent was obtained from the patient.

PERMISSION TO REPRODUCE MATERIAL FROM OTHER SOURCES

N/A.

CLINICAL TRIAL REGISTRATION (INCLUDING TRIAL NUMBER)

N/A.

ORCID

Kazuhisa Chonabayashi https://orcid.org/0000-0003-4825-5857
Yoshinori Yoshida https://orcid.org/0000-0001-5511-9090

REFERENCES

1. Claringbould A, Zaugg JB. Enhancers in disease: molecular basis and emerging treatment strategies. Trends Mol Med. 2021;27(11):1060–73.
2. Northcott PA, Lee C, Zichner T, Stütz AM, Erkek S, Kawauchi D, et al. Enhancer hijacking activates GFI1 family oncogenes in medulloblastoma. Nature. 2014;511(7510):428–34.
3. Taub R, Kirsch I, Morton C, Lenoir G, Swan D, Tronick S, et al. Translocation of the c-myc gene into the immunoglobulin heavy chain locus in human Burkitt lymphoma and murine plasmacytoma cells. Proc Natl Acad Sci U S A. 1982;79(24):7837–41.
4. Cleary ML, Sklar J. Nucleotide sequence of a *t*(14;18) chromosomal breakpoint in follicular lymphoma and demonstration of a breakpoint-cluster region near a transcriptionally active locus on chromosome 18. Proc Natl Acad Sci U S A. 1985;82(21):7439–43.
5. Gröschel S, Sanders MA, Hoogenboezem R, de Wit E, Bouwman BAM, Erpelinck C, et al. A single oncogenic enhancer rearrangement causes concomitant EVI1 and GATA2 deregulation in leukemia. Cell. 2014;157(2):369–81.
6. Yamazaki H, Suzuki M, Otsuki A, Shimizu R, Bresnick EH, Engel JD, et al. A remote GATA2 hematopoietic enhancer drives leukemogenesis in inv(3)(q21;q26) by activating EVI1 expression. Cancer Cell. 2014;25(4):415–27.
7. Lugthart S, Gröschel S, Beverloo HB, Kayser S, Valk PJ, van Zelderen-Bhola SL, et al. Clinical, molecular, and prognostic significance of WHO type inv(3)(q21q26.2)/*t*(3;3)(q21;q26.2) and various other 3q abnormalities in acute myeloid leukemia. J Clin Oncol. 2010;28(24):3890–8.
8. Rogers HJ, Vardiman JW, Anastasi J, Raca G, Savage NM, Cherry AM, et al. Complex or monosomal karyotype and not blast percentage is associated with poor survival in acute myeloid leukemia and myelodysplastic syndrome patients with inv(3)(q21q26.2)/*t*(3;3)(q21;q26.2): a bone marrow pathology group study. Haematologica. 2014;99(5):821–9.
9. Sasaki K, Montalban-Bravo G, Kanagal-Shamanna R, Jabbour E, Ravandi F, Kadia T, et al. Natural history of newly diagnosed myelodysplastic syndrome with isolated inv(3)/*t*(3;3). Am J Hematol. 2020;95(12):E326–e9.
10. Hu Z, Hu S, Ji C, Tang Z, Thakral B, Loghavi S, et al. 3q26/EVI1 rearrangement in myelodysplastic/myeloproliferative neoplasms: an early event associated with a poor prognosis. Leuk Res. 2018;65:25–8.
11. Ottema S, Mulet-Lazaro R, Beverloo HB, Erpelinck C, van Herk S, van der Helm R, et al. Atypical 3q26/MECOM rearrangements genocopy inv(3)/*t*(3;3) in acute myeloid leukemia. Blood. 2020;136(2):224–34.
12. Ottema S, Mulet-Lazaro R, Erpelinck-Verschueren C, van Herk S, Havermans M, Arricibita Varea A, et al. The leukemic oncogene EVI1 hijacks a MYC super-enhancer by CTCF-facilitated loops. Nat Commun. 2021;12(1):5679.
13. Tang G, Hu S, Wang SA, Xie W, Lin P, Xu J, et al. *T*(3;8)(q26.2;q24) often leads to MECOM/MYC rearrangement and is commonly associated with therapy-related myeloid neoplasms and/or disease progression. J Mol Diagn. 2019;21(2):343–51.
14. Xu X, Su M, Levy NB, Mohtashamian A, Monaghan S, Kaur P, et al. Myeloid neoplasm with *t*(3;8)(q26;q24): report of six cases and review of the literature. Leuk Lymphoma. 2014;55(11):2532–7.
15. Khoury JD, Solary E, Abla O, Akkari Y, Alaggio R, Apperley JF, et al. The 5th edition of the World Health Organization classification of Haematolymphoid Tumours: myeloid and histiocytic/dendritic neoplasms. Leukemia. 2022;36(7):1703–19.
16. Montefiori LE, Bendig S, Gu Z, Chen X, Pölönen P, Ma X, et al. Enhancer hijacking drives oncogenic BCL11B expression in lineage-ambiguous stem cell leukemia. Cancer Discov. 2021;11(11):2846–67.
17. Kubota S, Tokunaga K, Umezu T, Yokomizo-Nakano T, Sun Y, Oshima M, et al. Lineage-specific RUNX2 super-enhancer activates MYC and promotes the development of blastic plasmacytoid dendritic cell neoplasm. Nat Commun. 2019;10(1):1653.
18. Takahashi K, Tanabe K, Ohnuki M, Narita M, Ichisaka T, Tomoda K, et al. Induction of pluripotent stem cells from adult human fibroblasts by defined factors. Cell. 2007;131(5):861–72.
19. Kotini AG, Chang CJ, Boussaad I, Delrow JJ, Dolezal EK, Nagulapally AB, et al. Functional analysis of a chromosomal deletion associated with myelodysplastic syndromes using isogenic human induced pluripotent stem cells. Nat Biotechnol. 2015;33(6):646–55.
20. Garçon L, Ge J, Manjunath SH, Mills JA, Apicella M, Parikh S, et al. Ribosomal and hematopoietic defects in induced pluripotent stem cells derived from diamond Blackfan anemia patients. Blood. 2013;122(6):912–21.
21. Imamura K, Izumi Y, Watanabe A, Tsukita K, Woltjen K, Yamamoto T, et al. The Src/c-Abl pathway is a potential therapeutic target in amyotrophic lateral sclerosis. Sci Transl Med. 2017;9(391):eaaf3962.
22. Chao MP, Gentles AJ, Chatterjee S, Lan F, Reinisch A, Corces MR, et al. Human AML-iPSCs reacquire leukemic properties after differentiation and model clonal variation of disease. Cell Stem Cell. 2017;20(3):329–44.e7.
23. Okita K, Yamakawa T, Matsumura Y, Sato Y, Amano N, Watanabe A, et al. An efficient nonviral method to generate integration-free human-induced pluripotent stem cells from cord blood and peripheral blood cells. Stem Cells. 2013;31(3):458–66.
24. Voit RA, Tao L, Yu F, Cato LD, Cohen B, Fleming TJ, et al. A genetic disorder reveals a hematopoietic stem cell regulatory network co-opted in leukemia. Nat Immunol. 2023;24(1):69–83.
25. Bahr C, von Paleske L, Uslu VV, Remeseiro S, Takayama N, Ng SW, et al. A Myc enhancer cluster regulates normal and leukaemic haematopoietic stem cell hierarchies. Nature. 2018;553(7689):515–20.
26. Stathis A, Bertoni F. BET proteins as targets for anticancer treatment. Cancer Discov. 2018;8(1):24–36.
27. Yoshino S, Yokoyama T, Sunami Y, Takahara T, Nakamura A, Yamazaki Y, et al. Trib1 promotes acute myeloid leukemia progression by modulating the transcriptional programs of Hoxa9. Blood. 2021;137(1):75–88.
28. Morimoto S, Takahashi S, Fukushima K, Saya H, Suzuki N, Aoki M, et al. Ropinirole hydrochloride remedy for amyotrophic

lateral sclerosis - protocol for a randomized, double-blind, placebo-controlled, single-center, and open-label continuation phase I/IIa clinical trial (ROPALS trial). Regen Ther. 2019;11:143–66.
29. Imamura K, Izumi Y, Banno H, Uozumi R, Morita S, Egawa N, et al. Induced pluripotent stem cell-based drug repurposing for amyotrophic lateral sclerosis medicine (iDReAM) study: protocol for a phase I dose escalation study of bosutinib for amyotrophic lateral sclerosis patients. BMJ Open. 2019;9(12):e033131.
30. Kotini AG, Chang CJ, Chow A, Yuan H, Ho TC, Wang T, et al. Stage-specific human induced pluripotent stem cells map the progression of myeloid transformation to transplantable leukemia. Cell Stem Cell. 2017;20(3):315–28.e7.
31. Ye Z, Liu CF, Lanikova L, Dowey SN, He C, Huang X, et al. Differential sensitivity to JAK inhibitory drugs by isogenic human erythroblasts and hematopoietic progenitors generated from patient-specific induced pluripotent stem cells. Stem Cells. 2014;32(1):269–78.

SUPPORTING INFORMATION

Additional supporting information can be found online in the Supporting Information section at the end of this article.

How to cite this article: Nakamura M, Chonabayashi K, Narita M, Matsumura Y, Nishikawa M, Ochi Y, et al. Modelling and drug targeting of a myeloid neoplasm with atypical 3q26/*MECOM* rearrangement using patient-specific iPSCs. Br J Haematol. 2024;205(4):1430–1443. https://doi.org/10.1111/bjh.19720